

A Family of Single-Phase Single-Stage Boost Inverters

Sze Sing Lee ¹, Senior Member, IEEE, Ricxon Jie Sheng Lim,
 Reza Barzegarkhoo ², Graduate Student Member, IEEE, Chee Shen Lim ³, Senior Member, IEEE,
 Felipe Bovolini Grigoletto ⁴, Member, IEEE, and Yam Prasad Siwakoti ⁵, Senior Member, IEEE

Abstract—H-bridge inverter is a common topology used for single-phase applications. Due to its limited voltage gain, a two-stage power conversion with a front-end dc–dc converter is usually adopted to accommodate the low dc source voltage. Recently, single-stage boost inverters are gaining significant interest due to their higher power efficiency and compactness. In this article, we present a family of boost inverters with continuous dc source current. By the incorporation of merely a power switch and a boost inductor to the first leg of H-bridge, voltage boosting and three-level generation can be simultaneously achieved within a single-stage operation. All potential topologies using the same number of components are derived. An extension to generate five voltage levels with voltage gain enhancement is also proposed. The operation of the proposed boost inverters is thoroughly analyzed. The simulation and experimental results are presented for verification.

Index Terms—Boost inverters (BIs), H-bridge, multilevel inverters, single-stage.

I. INTRODUCTION

AN H-BRIDGE, which is also referred to as the full-bridge inverter, is a classical topology that has been widely used in single-phase applications. With merely four power switches, it is capable to generate three ac voltage levels while ensuring bidirectional power conversion between the dc and ac sides at the same time. An H-bridge is a buck-type inverter with its dc to ac voltage gain controllable up to unity by regulating

Manuscript received 11 May 2022; revised 26 July 2022 and 27 August 2022; accepted 9 October 2022. Date of publication 25 October 2022; date of current version 15 March 2023. (Corresponding author: Sze Sing Lee.)

Sze Sing Lee is with the Newcastle University in Singapore, Singapore 567739 (e-mail: ss.lee@ieee.org).

Ricxon Jie Sheng Lim is with the Newcastle University in Singapore, Singapore 567739, and also with the Singapore Institute of Technology, Singapore 138683 (e-mail: 1901384@sit.singaporetech.edu.sg).

Reza Barzegarkhoo and Yam Prasad Siwakoti are with the Faculty of Engineering and Information Technology, University of Technology Sydney, Sydney, NSW 2007, Australia (e-mail: reza.barzegarkho@student.uts.edu.au; yam.siwakoti@uts.edu.au).

Chee Shen Lim is with the School of Advanced Technology, Xi'an Jiaotong-Liverpool University, Suzhou 215123, China (e-mail: cheeshen.lim@xjtlu.edu.cn).

Felipe Bovolini Grigoletto is with the Federal University of Pampa (UNIPAMPA), Alegrete 97546-550, Brazil (e-mail: felipegrigoletto@unipampa.edu.br).

Color versions of one or more figures in this article are available at <https://doi.org/10.1109/TIE.2022.3215827>.

Digital Object Identifier 10.1109/TIE.2022.3215827

the modulation index of the sinusoidal pulsewidth modulation (PWM). For applications that require voltage boosting, such as grid-connected renewable energy or energy storage systems, a front-end dc–dc boost converter is usually mandatory to provide a sufficient dc-link voltage for the H-bridge inverter [1], [2]. A main downside of this two-stage power conversion structure is its low efficiency due to the high loss dissipation across the boost converter. The efficiency can be improved by making use of two paralleled front-end boost converters so that the interleaving operation between the two converters [3], [4] provides equal power sharing to reduce the losses in the dc–dc stage.

Instead of improving the two-stage topologies, significant research has been devoted to establishing single-stage inverters that inherit high-voltage-boosting capability. In [5] and [6], the positive terminal of an H-bridge is disconnected to constitute two boost converters with separate dc links. In order to prevent from dc offsets in the ac output, both converters are controlled with a sinusoidal varying duty cycle that not only generates a differential ac voltage but also enables their dc voltages to counteract each other at the same time. It is important to note that the generation of accurate differential ac voltage between the two dc links is highly complicated, rendering the design of control scheme for this topology challenging [7]. Moreover, the circulating current is another major concern that needs to be addressed.

Impedance-source inverters are another type of single-stage topologies that also gain popularity in recent years [8]. The earliest impedance-source inverter introduced in 2003 is referred to as a Z-source inverter [9]. As its name implies, a Z-shaped impedance network is integrated into the dc link of the conventional voltage-source inverter. Note that a shoot-through state is introduced when both switches in the same phase leg are ON, thereby allowing the impedance network to operate with a boosted dc-link voltage. Despite the drawbacks, such as a discontinuous input current and the need of several passive components for the impedance network, this pioneering contribution has inspired substantial related research works. A comprehensive review concerning the developments of impedance-source inverters can be found in [10], [11], and [12].

Recently, a distinctive family named split-source inverter (SSI) that features simplicity, high compactness, continuous input dc current, and continuous dc-link voltage has been explored [13], [14], [15], [16], [17]. It requires the incorporation of only one inductor, one capacitor, and two diodes into the

H-bridge inverter. The single-stage configuration, which encompasses a boost converter, and an H-bridge inverter permit concurrent accomplishment of dc-link voltage boosting and ac voltage generation. The first topology introduced in [13] is later denoted as SSI in [14] to better reflect the circuit structure. A more compact design can be attained by relocating the dc source with the utilization of a commercial device that comprises two common-cathode diodes [18]. All the earlier SSIs, however, exhibit common shortcomings, such as high-frequency commutations of diodes, aggravated harmonics that are induced by the variable charging duty cycle of the boost inductor, and incapability of bidirectional power conversion.

A latter study improves the SSI by replacing the two diodes with two power MOSFETs [19]. When both the power MOSFETs operate in synchronous rectification mode at the line frequency, the modified SSI mitigates the high-frequency commutation of diodes and achieves bidirectional power flow. Besides, the presented hybrid quasi-sinusoidal and constant PWM scheme is able to provide a constant charging duty cycle for the boost inductor. It is also worth noting that the operations of the two H-bridge legs are effectively decoupled. One leg is responsible for inductor charging and dc-link voltage control, while the other leg is responsible for ac voltage generation according to the sinusoidal PWM.

A single-phase SSI topology that allows bidirectional power flow with reduced component count is presented in [20]. While preserving all the inherent merits of earlier SSIs, this so-called simplified SSI exhibits the highest compactness in the SSI family. Voltage boost function and three voltage levels generation are attained within a single-stage operation by merely the incorporation of an additional power switch into the first leg of an H-bridge. However, this topology suffers from high-frequency common-mode voltage (CMV) that is not feasible for applications, such as photovoltaic (PV) system.

By using the same number of components, all potential topologies for single-stage boost inverters (BIs) are derived in this article. Some of the topologies in this BI family have been presented in the literature, while the remaining are novel. An extension from three- to five-level generation with voltage gain enhancement is also proposed. The rest of this article is organized as follows. In Section II, the BI family is introduced. Section III presents an extension to generate five voltage level and enhance voltage gain. Section IV compares the proposed topology with the state-of-the-art five-level inverters. The simulation and experimental results are discussed in Section V. Finally, Section VI concludes this article.

II. THREE-LEVEL BIS

Fig. 1 depicts the derivation of the BI family. Four basic topologies of the dc–dc boost converter are considered, and they are termed as BC1–BC4. By combining BCs with a similar circuit structure for their dc source and boost inductor, a total of six switched-boost cells (SBC1–SBC6) are obtained. In each SBC, a power switch is inserted into the half-bridge that introduces a new switching state for controlling the voltage of ac neutral. Six topologies of BI (BI1–BI6) are established by

adding a half-bridge to each respective SBC. The first (BI1) and third (BI3) topology, as depicted in Fig. 1, has been introduced in [20] and [21], respectively, while the remaining BIs are novel that have not been presented in the literature.

All BIs, as depicted in Fig. 1, can generate three voltage levels and boosting voltage gain simultaneously within a single-stage operation. They have four useful switching states, as shown in Fig. 2. The boost inductor can be charged by clamping it across the dc source during all voltage levels. To boost the voltage across capacitor, the boost inductor is discharged in series with the dc source during zero level.

To enable a single-stage dc–ac power conversion, PWM scheme, as depicted in Fig. 3, consists of two reference signals and a triangular carrier. A constant duty cycle D for charging the boost inductor is obtained by comparing the constant reference V_{const} with the triangular carrier. By considering the volt-second balance of the boost inductor, the voltage across capacitor V_C is

$$V_C = \frac{1}{1-D} V_{\text{dc}}. \quad (1)$$

Simultaneously, a sinewave reference is used to control the ac output with the amplitude of fundamental voltage as follows:

$$\hat{V}_{\text{on},1} = M V_C = \frac{M}{1-D} V_{\text{dc}} \quad (2)$$

where $M = \hat{V}_{\text{sine}}/\hat{V}_{\text{tri}}$ is the modulation index. In this PWM scheme, the modulation index and constant duty cycle are coupled for achieving voltage boosting and ac voltage generation simultaneously in a single-stage operation. The minimum value for constant reference is given by the peak of sinewave reference. Therefore, the minimum constant duty cycle is equal to the inverter modulation index, $D_{\text{min}} = M$.

The ripple of capacitor voltage and ripple of inductor current consist of double-line-frequency and high-frequency components. A comprehensive ripple analysis can be referred to the article presented in [20]. Considering sinusoidal ac current, the capacitor voltage ripple ΔV_C and inductor current ripple ΔI_L can be, respectively, written as

$$\Delta V_C = \frac{M \hat{I}_{o,1}}{4\pi f_o C} + \frac{D(1-D) I_L}{C f_s} \quad (3)$$

$$\Delta I_L = \frac{M \hat{I}_{o,1} (1-D)}{16\pi^2 f_o^2 L C} + \frac{D V_{\text{dc}}}{L f_s} \quad (4)$$

where $\hat{I}_{o,1}$ is the amplitude of fundamental ac current, I_L is the average dc source or inductor current, f_o is the fundamental ac frequency, f_s is the frequency of the triangular carrier, L is the inductance, and C is the capacitance.

III. EXTENDED FIVE-LEVEL TOPOLOGY WITH VOLTAGE GAIN ENHANCEMENT

All BIs, as depicted in Fig. 1, have the same component count and operating principle, as summarized in Fig. 2. The location of ac neutral point that determines the inverter CMV is their main distinctive feature. The ac neutral point of BI1, BI2, BI4,

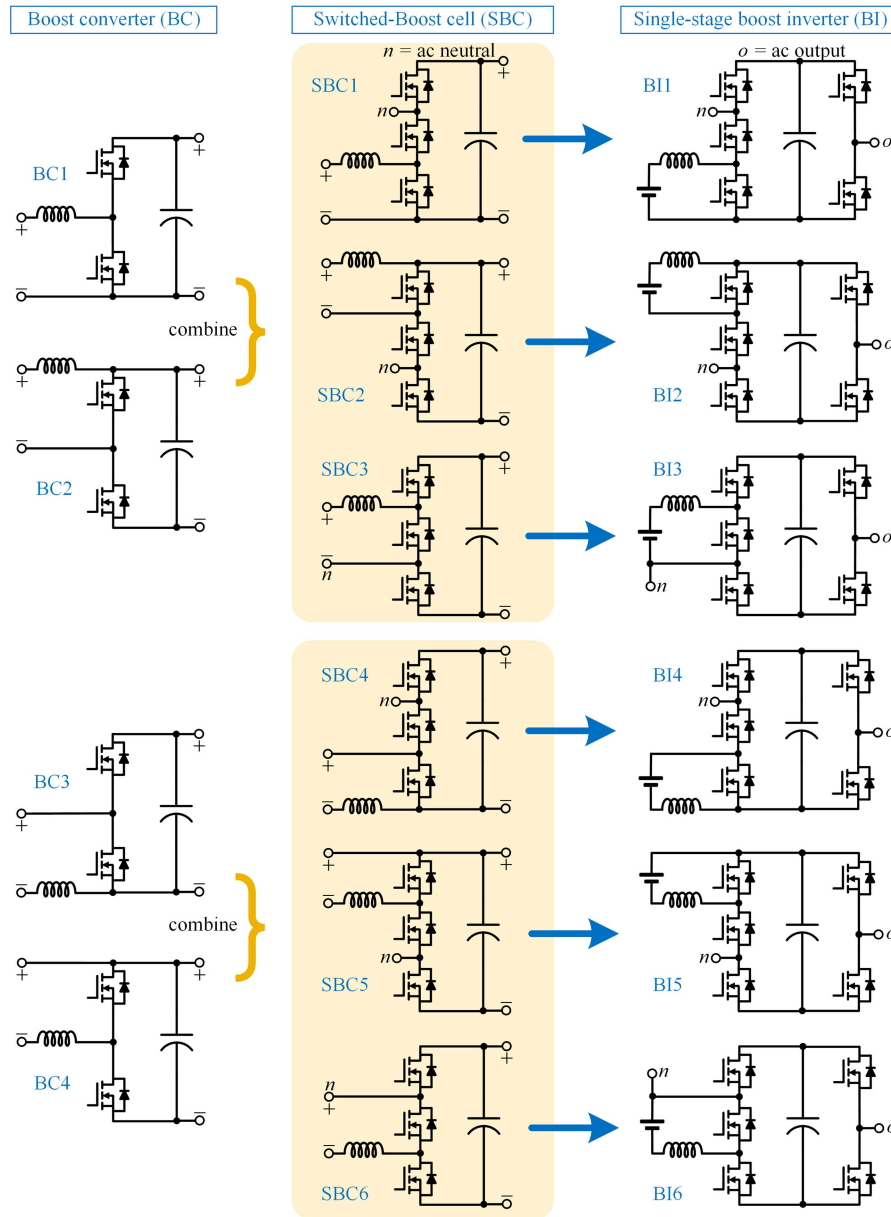


Fig. 1. Derivation of single-phase single-stage three-level BIs.

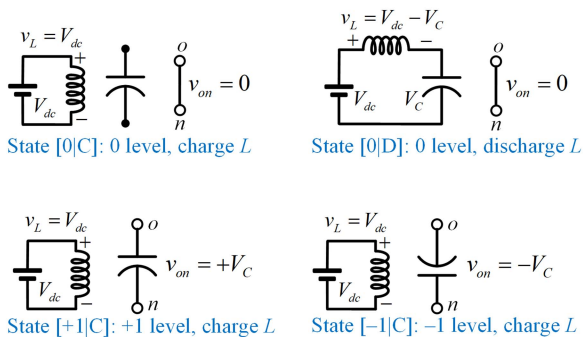


Fig. 2. Generalized switching states of three-level BIs.

and BI5 is separated from the dc source by a switch. Due to the switching of this switch, high-frequency CMV is introduced.

Among the novel three-level BIs in Fig. 1, BI6 has an attractive structure when its ac neutral is directly connected to the positive terminal of the dc source. This implies that the neutral point voltage with respect to any dc source terminals is constant without high-frequency CMV. As shown in Fig. 4(a), the CMV across the parasitic capacitor is $-V_{dc}$, which is constant. It prevents the risk of leakage current that is very feasible for applications, such as PV system. Therefore, this topology is considered for further extension.

To increase the number of voltage levels from three to five, a capacitor C_2 and four power switches S6–S9 are added, as shown in Fig. 4(b). Fig. 5 shows the switching states of the extended five-level topology [BI6(5L)]. Both capacitors C_1 and C_2 are

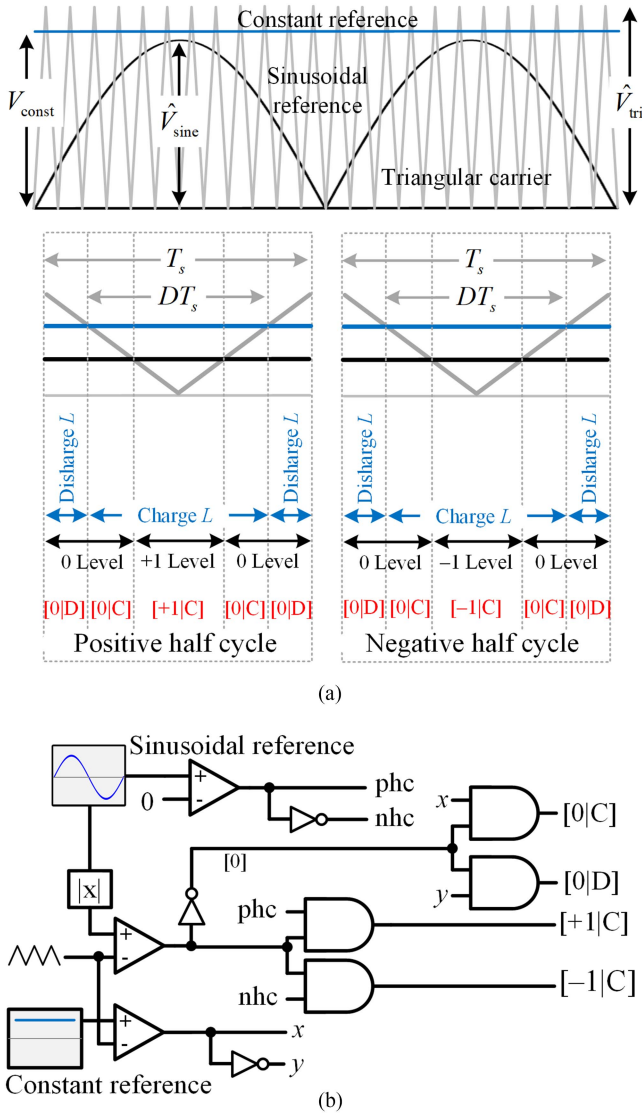


Fig. 3. PWM scheme of three-level BIs. (a) Key waveforms. (b) PWM unit.

charged in parallel. Therefore, their voltage is equal. Maximum voltage levels (+2 and -2) can be generated by discharging the capacitors in series. The magnitude of these maximum voltage levels is two times of the capacitor voltage. This implies that the voltage gain of BI6(5L) is double compared with BI6 for the same D and M .

As shown in Fig. 5, the boost inductor can be charged during any voltage levels. To discharge the boost inductor during 0, +1, or -1 level that ensures a constant duty cycle D for voltage boosting while simultaneously generating five-level ac voltage, a phase-shifted PWM scheme, as depicted in Fig. 6, is proposed. This PWM scheme not only enables a five-level generation that reduces the overall total harmonic distortion (THD) of ac output voltage but it also improves the harmonic spectrum. Compared with BI6, the dominant harmonics of ac voltage generated by BI6(5L) is extended to twice the triangular carrier frequency. This is beneficial for reducing the power filter requirement, i.e., smaller power filter for higher cutoff frequency.

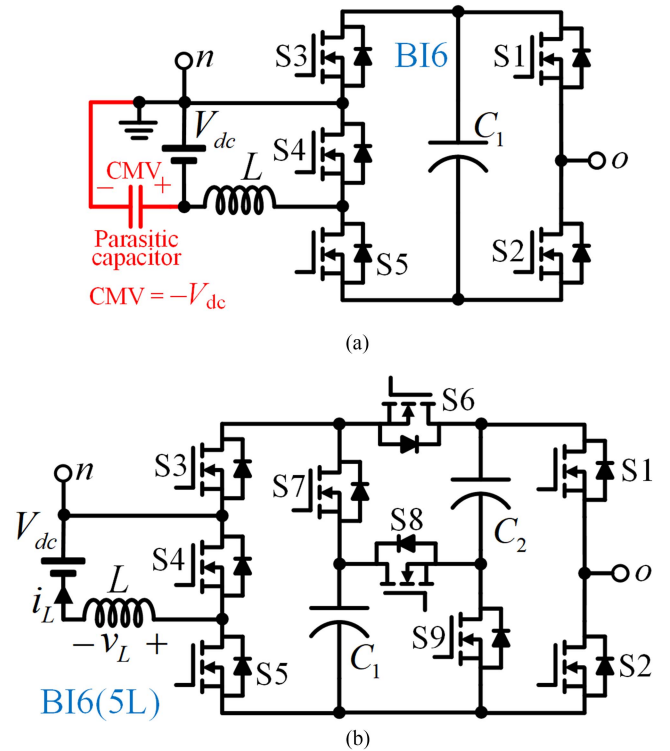


Fig. 4. Proposed BIs. (a) Three-level BI (BI6) without high-frequency CMV. (b) Extension of BI6 with five-level generation and voltage gain enhancement.

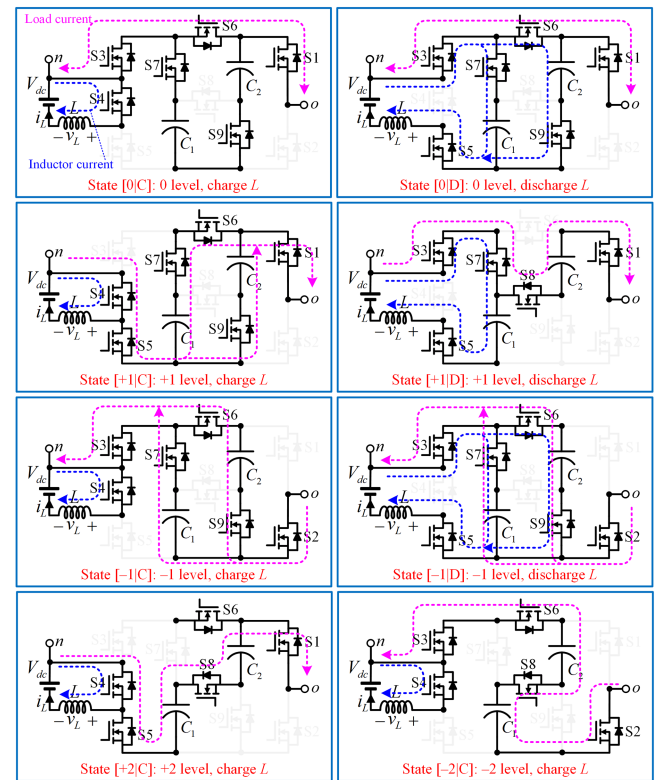


Fig. 5. Switching states of extended five-level BI [BI6(5L)].

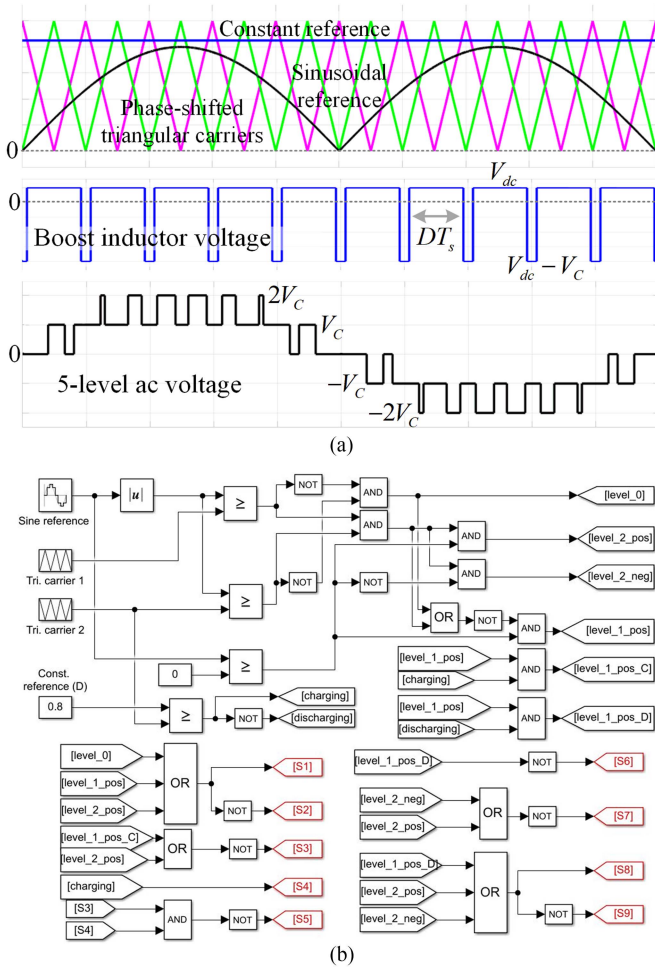


Fig. 6. Phase-shifted PWM scheme of extended five-level BI [BI(5L)]. (a) Key waveforms. (b) Implementation of PWM scheme.

To design BI6(5L), $D_{\min} = M$ is considered. Modulation index M for the required voltage gain G is

$$M = \frac{G}{G + 2}. \quad (5)$$

Two capacitors with the same value are considered as follows:

$$C_1 = C_2 = C = \frac{1}{\Delta V_C} \left(\frac{M \hat{I}_{o,1}}{4\pi f_o} + \frac{D(1-D)I_L}{f_s} \right). \quad (6)$$

Finally, the value of inductor can be calculated as follows:

$$L = \frac{1}{\Delta I_L} \left(\frac{M \hat{I}_{o,1} (1-D)}{16\pi^2 f_o^2 C} + \frac{D V_{dc}}{f_s} \right). \quad (7)$$

IV. COMPARISON WITH EXISTING FIVE-LEVEL BIs

Table I summarizes the comparison of the proposed BI6(5L) with the state-of-the-art five-level inverters without high-frequency CMV. The topologies presented in [22], [23], [24], and [25] uses lesser number of power switches. However, their major drawbacks are limited voltage gain and discontinuous dc source current. A five-level inverter presented in [26] improved

TABLE I
COMPARISON BETWEEN THE PROPOSED BI6(5L) AND THE EXISTING FIVE-LEVEL INVERTERS WITHOUT HIGH-FREQUENCY CMV

Topology	N_S	N_D	N_C	N_L	G	CIC
[22]	6	1	2	0	M	No
[23]	6	2	2	0	$2M$	No
[24]	7	2	2	0	$2M$	No
[25]	6	2	2	0	$2M$	No
[26]	10	0	2	1	$2M/(1-D)$	Partial
BI6(5L)	9	0	2	1	$2M/(1-D)$	Yes

N_S = number of switches, N_D = number of diodes, N_C = number of capacitors, N_L = number of inductors, G = voltage gain, M = modulation index, D = duty-cycle, and CIC = continuous input current.

the voltage gain significantly, however, with a tradeoff of high switch count. In addition, the issue of discontinuous dc source current is not fully resolved. The capacitors of this topology are connected in series. They are individually charged by the boost inductor and requires voltage balancing control that unfortunately causes significant distortion to the inductor current due to limited redundant states. Inductor or dc source current with discontinuous and highly distorted waveform increases the overall rms value. Referring to the superposition theorem: $I_{\text{rms}}^2 = I_{\text{dc}}^2 + I_{1,\text{rms}}^2 + I_{2,\text{rms}}^2 + \dots$, where I_{rms} is the overall rms current, I_{dc} is the average current, $I_{1,\text{rms}}$ is the rms current of the fundamental harmonic, etc., and the overall rms current would be significantly higher than the average current that increases power loss. This results in lower efficiency because the average power delivered by the inverter is contributed by the average current only. In addition, discontinuous dc source current is not feasible for applications, such as PV system. The proposed BI6(5L) provides the best performance that achieved high voltage gain and continuous dc source current while saving one switch count compared with the article presented in [26]. In addition, the number of conducting switches for inductor current in the proposed topology is also lesser than the article presented in [26].

V. SIMULATION AND EXPERIMENTAL RESULTS

Simulations were conducted using MATLAB/Simulink to verify the operation of the proposed BI6 and BI(5L). To compare the performance of both topologies, the same parameters are considered: $V_{\text{dc}} = 100$ V, $D = M = 0.8$, $C_1 = C_2 = 1000$ μF , $L = 1$ mH, $f_s = 10$ kHz, $f_o = 50$ Hz, load resistance = 100 Ω , and load inductance = 100 mH.

By charging the boost inductor with a constant duty cycle of 0.8, the voltage of each capacitor in both topologies is boosted to 500 V. Three symmetrical voltage levels are generated by BI6 between 500 and -500 V and the amplitude of fundamental component is 400 V. The BI6(5L) has clear improvement that generates two additional voltage levels, i.e., $+1000$ V and -1000 V. With the same modulation index of 0.8, the amplitude of fundamental ac voltage generated by BI6(5L) is 800 V, double compared with BI6. Consequently, the output power of BI6(5L) in Fig. 7 is 2914 W, which is four times higher than 730 W of BI6. In addition, the fast Fourier transform (FFT) of ac voltage shows that the dominant harmonics of BI6(5L) are

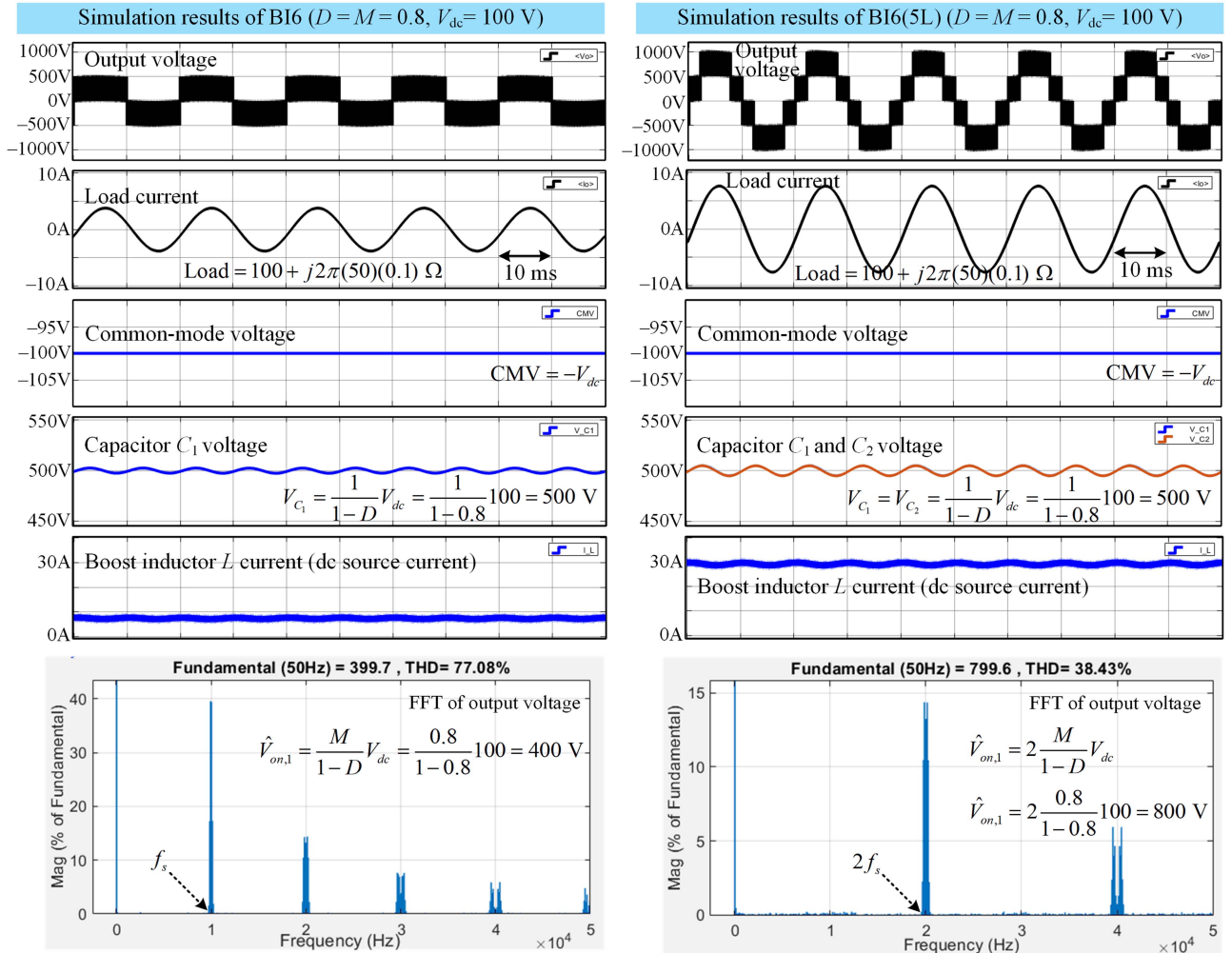


Fig. 7. Simulation results of the proposed BI6 and BI6(5L).

concentrated at 20 kHz that is twice compared with 10 kHz of BI6. In addition, the harmonics magnitude and overall THD of BI6(5L) are significantly lower that can improve the load current quality. These significant improvements are achieved while retaining the advantages of BI6, such as constant CMV, without high-frequency component and continuous dc source current.

For further verification, a low power (200 W) proof-of-concept experimental prototype for BI6(5L) was implemented using silicon carbide MOSFETs (C3M0120090D) that have the ON-state resistance of 120 m Ω . The experimental prototype, as depicted in Fig. 8, was implemented to verify the operation of the proposed topology. The same parameters in simulation study were used, except V_{dc} was reduced to 22 V to ensure that the dc source current is within 10-A current limit of the power supply. Table II summarizes the simulation and experimental parameters of BI6(5L). Phase-shifted PWM scheme, as presented in Fig. 6, was implemented in PLECS and switching signals were generated in real time using the RT Box controller.

Fig. 9(a) shows the measured steady-state response at $D = M = 0.8$ under both R and RL load. It is clearly seen

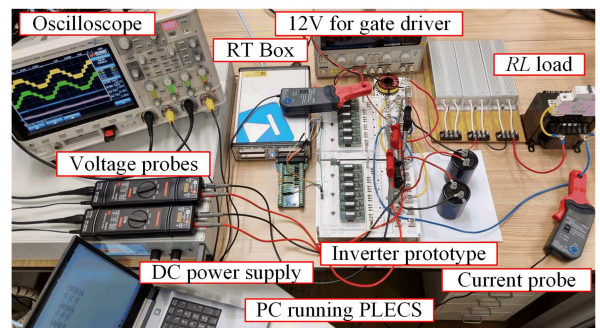


Fig. 8. Experimental setup.

that the dc source or boost inductor L current is continuous. Zoomed-in to this current shows the charging and discharging duration of the inductor is 80 μ s and 20 μ s, respectively, that confirms the operating duty cycle (0.8) and frequency (10 kHz). The average voltage across both C_1 and C_2 is boosted to 110 V. By connecting these capacitors in series during $[+2]C$ state, the maximum voltage level generated by the BI6(5L) at $D = 0.8$

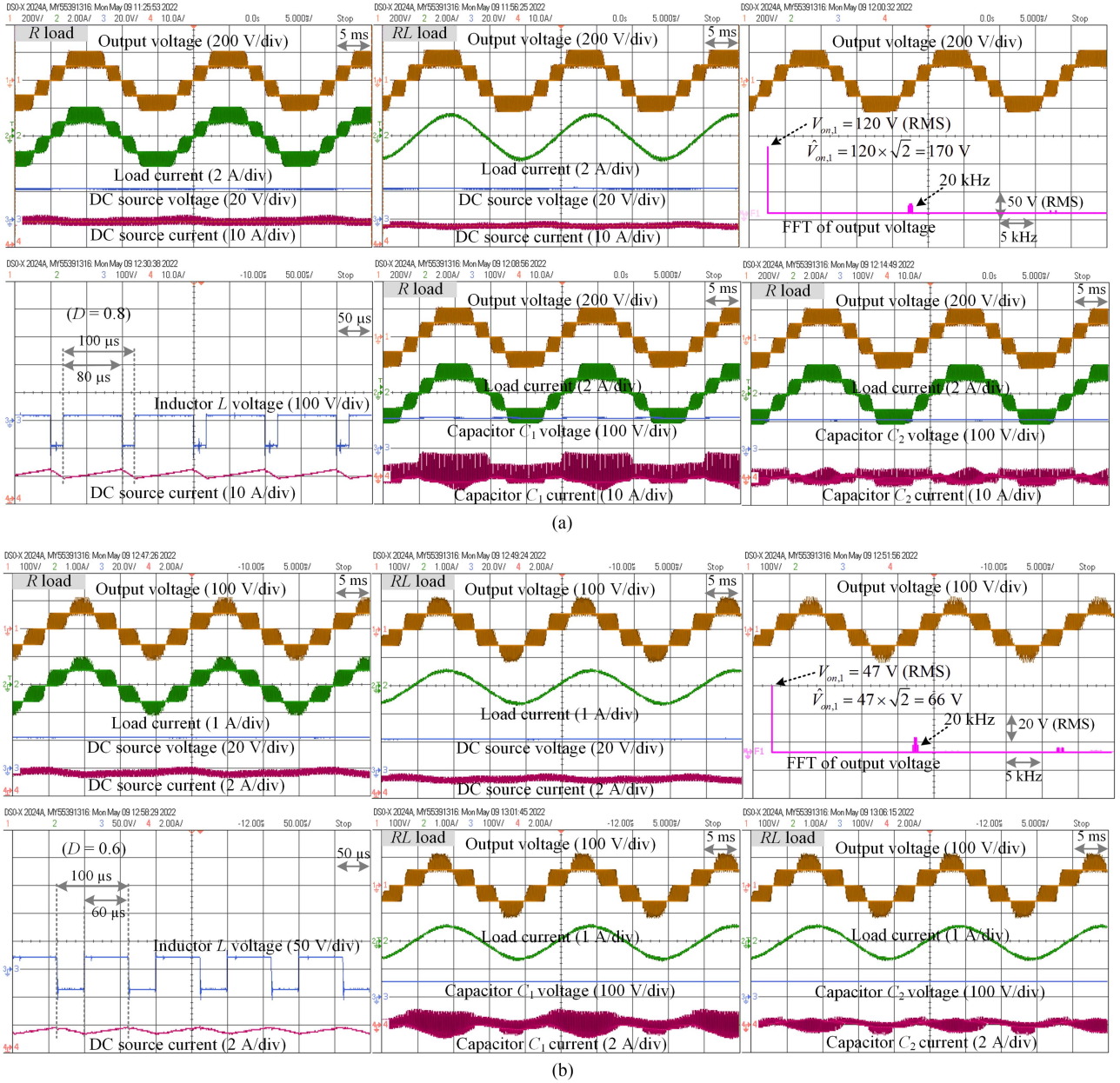


Fig. 9. Measured steady-state response at (a) $D = M = 0.8$ and (b) $D = M = 0.6$.

TABLE II
SIMULATION AND EXPERIMENTAL PARAMETERS OF BI6(5L)

Parameter	Simulation	Experiment
Boost inductor, L	1 mH	1 mH
Capacitor, $C_1 = C_2 = C$	1000 μ F	1000 μ F
Carrier frequency, f_s	10 kHz	10 kHz
Output frequency, f_o	50 Hz	50 Hz
Input voltage, V_{dc}	100 V	22 V
Output voltage, $\hat{V}_{on,1}$	800 V	176 V
(at $D = M = 0.8$)		
Output power, P_o	2914 W	200 W

is 220 V, which is ten times higher than the dc source voltage. Five symmetrical voltage levels are observed in the ac output

voltage between 220 and -220 V. The fundamental component of the ac voltage is 120 V rms, as reflected by the spectrum captured from the FFT analysis. This observation matches well with the theoretical finding, and it is only slightly less than the calculated value of 124 V rms. The measured voltage gain is $170/22 = 7.7$, which is very close to the theoretical value of 8. The dominant harmonics of ac voltage are concentrated at 20 kHz that shows good agreement with the theoretical analysis and simulation results.

Experiments were repeated for $D = M = 0.6$ when the steady-state responses are summarized in Fig. 9(b). The inductor L is charged by the dc source for 60μ s and discharging to the capacitors for the remaining period in each switching cycle. Continuous inductor current is ensured while boosting

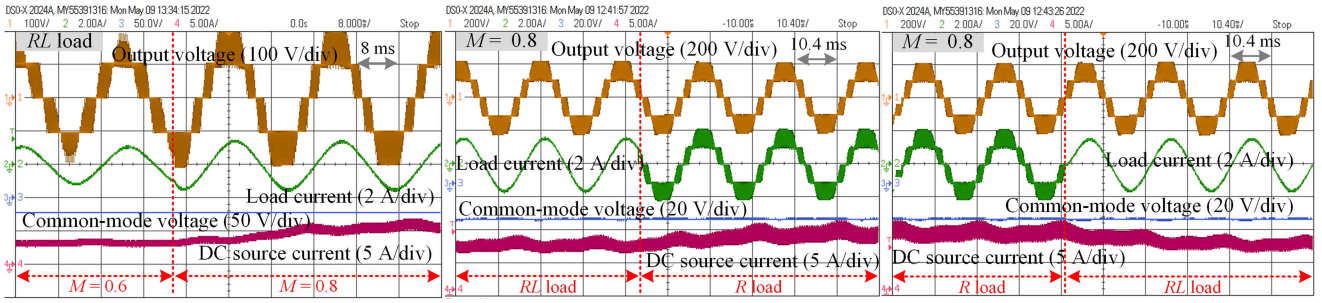


Fig. 10. Measured transient response.

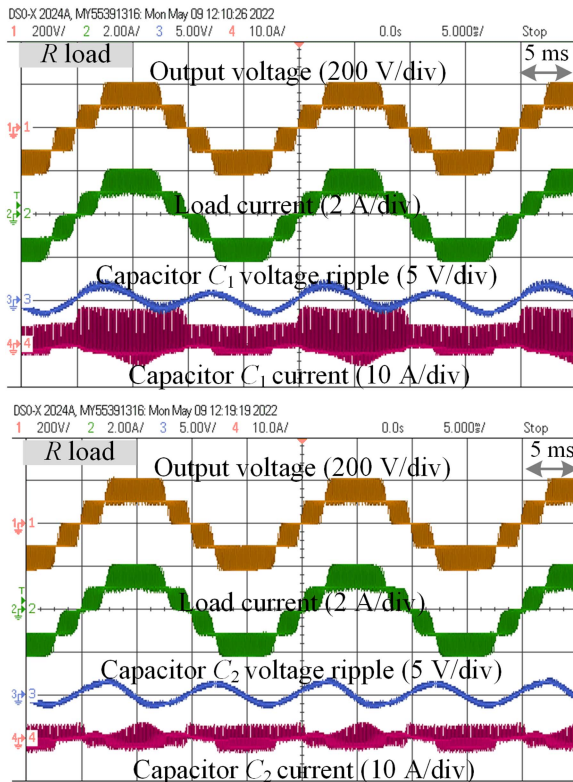


Fig. 11. Measured capacitors' voltage ripple of the proposed BI6(5L) at $M = D = 0.8$.

the dc source voltage from 22 to 55 V across each capacitor. The ac output voltage consists of five symmetrical voltage levels between 110 and -110 V. The measured peak of fundamental ac voltage is 66 V that verified the theoretical value: $\hat{V}_{on,1} = 2MV_{dc}/(1-D) = 2(0.6)(22)/(1-0.6) = 66$ V.

Fig. 10 shows the transient response of the BI6(5L) prototype. The increase in modulation index increases the magnitude of load current due to higher magnitude ac voltage. The load current changes instantly when the load is switched from R to RL load and vice-versa. The five-level waveform of the output voltage is maintained without any deterioration during the load transient. The CMV between the negative terminal of dc source and ac neutral is constant, i.e., -22 V. This verified the capability of the proposed BI6(5L) in mitigating high-frequency CMV.

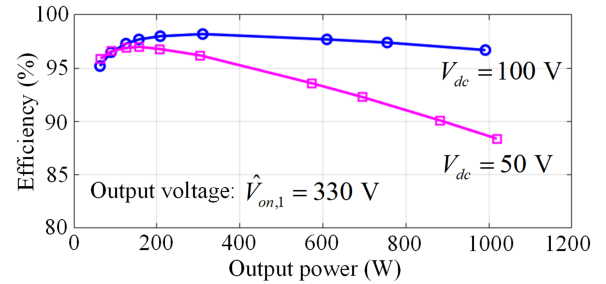


Fig. 12. Efficiency of the proposed BI6(5L).

The voltage ripple of capacitors C_1 and C_2 was also measured, as shown in Fig. 11. The ripple waveforms are in phase and similar because the capacitors are charged in parallel that balances their voltage naturally. The measured voltage ripple is approximately 3 V that is slightly higher than 2.4 V calculated using (3). Fig. 12 continues to investigate the efficiency of the proposed topology by modeling the experimental prototype in simulation. Considering a peak ac output voltage of 330 V and dc source voltages of 100 V and 50 V, peak efficiency exceeding 98% can be achieved. The efficiency decreases with power level and more apparent reduction is observed for 50 V due to higher dc source current.

VI. CONCLUSION

A family of six three-level BIs was derived in this article. They are the most compact topologies for single-phase single-stage boost dc-ac power conversion that consists of only five power switches, one capacitor, and one inductor. One of the three-level BIs without high-frequency CMV was further extended to generate five voltage levels. The proposed BI6(5L) also enhanced voltage gain in addition to retaining the benefit of continuous dc source current. In addition, a phase-shifted PWM scheme was proposed that enabled the simultaneous generation of five voltage levels and voltage boosting within a single-stage operation and extended the frequency of dominant harmonics in ac voltage. Good agreement among analysis, simulation, and experimental results had verified the operation and feasibility of the proposed BI6 and BI(5L).

REFERENCES

- [1] S. B. Kjaer, J. K. Pedersen, and F. Blaabjerg, "A review of single-phase grid-connected inverters for photovoltaic modules," *IEEE Trans. Ind. Appl.*, vol. 41, no. 5, pp. 1292–1306, Sep./Oct. 2005.
- [2] A. Sangwongwanich, Y. Yang, and F. Blaabjerg, "A sensorless power reserve control strategy for two-stage grid-connected PV systems," *IEEE Trans. Power Electron.*, vol. 32, no. 11, pp. 8559–8569, Nov. 2017.
- [3] Z. Zhao, M. Xu, Q. Chen, J.-S. Lai, and Y. Cho, "Derivation, analysis, and implementation of a boost–buck converter-based high-efficiency PV inverter," *IEEE Trans. Power Electron.*, vol. 27, no. 3, pp. 1304–1313, Mar. 2012.
- [4] Z. Zhao, J.-S. Lai, and Y. Cho, "Dual-mode double-carrier-based sinusoidal pulse width modulation inverter with adaptive smooth transition control between modes," *IEEE Trans. Ind. Electron.*, vol. 60, no. 5, pp. 2094–2103, May 2013.
- [5] R. O. Caceres and I. Barbi, "A boost DC–AC converter: Analysis, design, and experimentation," *IEEE Trans. Power Electron.*, vol. 14, no. 1, pp. 134–141, Jan. 1999.
- [6] M. Jang, M. Ciobotaru, and V. G. Agelidis, "A single-phase grid-connected fuel cell system based on a boost-inverter," *IEEE Trans. Power Electron.*, vol. 28, no. 1, pp. 279–288, Jan. 2013.
- [7] P. Sanchis, A. Ursæa, E. Gubía, and L. Marroyo, "Boost DC–AC inverter: A new control strategy," *IEEE Trans. Power Electron.*, vol. 20, no. 2, pp. 343–353, Mar. 2005.
- [8] J. Ma, H. Liu, J. Chen, Y. Li, and P. C. Loh, "A family of coupled dual-winding impedance-source inverters with continuous input currents and no DC-link voltage spikes," *IEEE J. Emerg. Sel. Topics Power Electron.*, to be published, doi: [10.1109/JESTPE.2020.3034394](https://doi.org/10.1109/JESTPE.2020.3034394).
- [9] F. Z. Peng, "Z-source inverter," *IEEE Trans. Ind. Appl.*, vol. 39, no. 2, pp. 504–510, Mar./Apr. 2003.
- [10] O. Ellabban and H. Abu-Rub, "Z-source inverter: Topology improvements review," *IEEE Ind. Electron. Mag.*, vol. 10, no. 1, pp. 6–24, Mar. 2016.
- [11] Y. P. Siwakoti, F. Z. Peng, F. Blaabjerg, P. C. Loh, and G. E. Town, "Impedance-source networks for electric power conversion—Part I: A topological review," *IEEE Trans. Power Electron.*, vol. 30, no. 2, pp. 699–716, Feb. 2015.
- [12] Y. P. Siwakoti, F. Z. Peng, F. Blaabjerg, P. C. Loh, G. E. Town, and S. Yang, "Impedance-source networks for electric power conversion—Part II: Review of control and modulation techniques," *IEEE Trans. Power Electron.*, vol. 30, no. 4, pp. 1887–1906, Apr. 2015.
- [13] H. Ribeiro, A. Pinto, and B. Borges, "Single-stage DC–AC converter for photovoltaic systems," in *Proc. IEEE Energy Convers. Congr. Expo.*, 2010, pp. 604–610.
- [14] A. Abdelhakim, P. Mattavelli, and G. Spiazzi, "Three-phase split-source inverter (SSI): Analysis and modulation," *IEEE Trans. Power Electron.*, vol. 31, no. 11, pp. 7451–7461, Nov. 2016.
- [15] L. A. Rodrigues, G. S. da Silva, and F. B. Grigoletto, "Control of split-source cascaded multilevel inverter (SS-CMI) for single-phase grid-connected photovoltaic systems," in *Proc. IEEE PES Innov. Smart Grid Technol. Conf. - Latin Amer.*, 2019.
- [16] A. Nahavandi, M. Roostae, and M. R. Azizi, "Single stage DC–AC boost converter," in *Proc. IEEE 7th Power Electron., Drive Syst. Technol. Conf.*, 2016, pp. 362–366.
- [17] F. Akbar, H. Cha, H. F. Ahmed, and A. A. Khan, "A family of single-stage high-gain dual-buck split-source inverters," *IEEE J. Emerg. Sel. Topics Power Electron.*, vol. 8, no. 2, pp. 1701–1713, Jun. 2020.
- [18] A. Abdelhakim, P. Mattavelli, P. Davari, and F. Blaabjerg, "Performance evaluation of the single-phase split-source inverter using an alternative DC–AC configuration," *IEEE Trans. Ind. Electron.*, vol. 65, no. 1, pp. 363–373, Jan. 2018.
- [19] S. S. Lee and Y. E. Heng, "Improved single-phase split-source inverter with hybrid quasi-sinusoidal and constant PWM," *IEEE Trans. Ind. Electron.*, vol. 64, no. 3, pp. 2024–2031, Mar. 2017.
- [20] S. S. Lee, A. S. T. Tan, D. Ishak, and R. Mohd-Mokhtar, "Single-phase simplified split-source inverter (S³I) for boost DC–AC power conversion," *IEEE Trans. Ind. Electron.*, vol. 66, no. 10, pp. 7643–7652, Oct. 2019.
- [21] X. Hu, P. Ma, B. Gao, and M. Zhang, "An integrated step-up inverter without transformer and leakage current for grid-connected photovoltaic system," *IEEE Trans. Power Electron.*, vol. 34, no. 10, pp. 9814–9827, Oct. 2019.
- [22] F. B. Grigoletto, "Five-level transformerless inverter for single-phase solar photovoltaic applications," *IEEE J. Emerg. Sel. Topics Power Electron.*, vol. 8, no. 4, pp. 3411–3422, Dec. 2020.
- [23] N. Vosoughi, S. H. Hosseini, and M. Sabahi, "A new transformer-less five-level grid-tied inverter for photovoltaic applications," *IEEE Trans. Energy Convers.*, vol. 35, no. 1, pp. 106–118, Mar. 2020.
- [24] R. Barzegarkhoo, Y. P. Siwakoti, and F. Blaabjerg, "A new switched-capacitor five-level inverter suitable for transformerless grid-connected applications," *IEEE Trans. Power Electron.*, vol. 35, no. 8, pp. 8140–8153, Aug. 2020.
- [25] R. Barzegarkhoo, Y. P. Siwakoti, N. Vosoughi, and F. Blaabjerg, "Six-switch step-up common-grounded five-level inverter with switched-capacitor cell for transformerless grid-tied PV applications," *IEEE Trans. Ind. Electron.*, vol. 68, no. 2, pp. 1374–1387, Feb. 2021.
- [26] R. Barzegarkhoo, S. S. Lee, Y. P. Siwakoti, S. A. Khan, and F. Blaabjerg, "Design, control, and analysis of a novel grid-interfaced switched-boost dual T-type five-level inverter with common-ground concept," *IEEE Trans. Ind. Electron.*, vol. 68, no. 9, pp. 8193–8206, Sep. 2021.



Sze Sing Lee (Senior Member, IEEE) received the B.Eng.(Hons.) and Ph.D. degrees in electrical engineering from Universiti Sains Malaysia, Gelugor, Malaysia, in 2010 and 2013, respectively.

From 2014 to 2019, he was a Lecturer/Assistant Professor with the University of Southampton Malaysia Campus, Malaysia. From 2018 to 2019, he was a Visiting Research Professor with Ajou University, South Korea. He is currently an Assistant Professor with Newcastle University, Singapore. His research interests include power converter/inverter topologies and their control strategies.

Dr. Lee was a recipient of the Outstanding Reviewer Award from the IEEE TRANSACTIONS ON POWER ELECTRONICS in 2020. He is an Associate Editor for IEEE TRANSACTIONS ON INDUSTRIAL ELECTRONICS and IEEE ACCESS, and a Guest Associate Editor for IEEE TRANSACTIONS ON POWER ELECTRONICS.



Ricxon Jie Sheng Lim is currently working toward the undergraduate joint degree in electrical power engineering with the Singapore Institute of Technology, Singapore, and Newcastle University in Singapore, Singapore.

His research interests include power system engineering, power electronics, and simulation modeling.



Reza Barzegarkhoo (Graduate Student Member, IEEE) received the B.S. degree from the University of Guilan, Rasht, Iran, in 2010, and the M.S. degree from the Sahand University of Technology, Tabriz, Iran, in 2012, both in electrical power engineering. He is currently working toward the Ph.D. degree with the Faculty of Engineering and Information Technology, University of Technology Sydney, Sydney, NSW, Australia.

From 2016 to 2019, he was with the Guilan Electrical Energy Distribution Company, Rasht, as a Senior Grid-Exploiting Electrical Power Engineer. From June to September 2022, he was a Guest Scientist with the Chair of Power Electronics, Christian-Albrechts-Universität zu Kiel (CAU) University, Kiel, Germany. He has authored and coauthored more than 40 journal/conference peer-review papers in the area of power electronics. His main research interests include the design and control of power electronic converters, multi-level voltage source inverters, switched-capacitor and switched-boost converters, photovoltaic transformerless grid-tied ac modules, and distributed generation systems.

Mr. Barzegarkhoo was the recipient of the prestigious Green Talent Award from the Federal Ministry of Education and Research, Germany, in 2021 and the "IES and PEDG Best Student Paper Awards" in 2022. He is a frequent Reviewer of several IEEE Transactions Journals in the area of power electronics. He was also selected as Distinguished Reviewer of 2020 by the IEEE Transactions on Industrial Electronics and Star Reviewer of 2021 by the Journal of Emerging and Selected Topics in Power Electronics.



Chee Shen Lim (Senior Member, IEEE) received the B.Eng.(Hons.) degree in electrical engineering from the University of Malaya, Kuala Lumpur, Malaysia, in 2009, and the joint-university Ph.D. degrees in power electronics and drives from the University of Malaya, and Liverpool John Moores University, Liverpool, U.K., in 2013.

From 2013 to 2015, he was a Research Scientist with Experimental Power Grid Centre, Agency for Science, Technology, and Research, Singapore. From 2015 to 2021, he was an Assistant/Associate Professor of electrical and electronic engineering with the University of Southampton Malaysia Campus. He is currently an Associate Professor of electrical and electronic engineering with Xi'an Jiaotong-Liverpool University, Suzhou, China.

Dr. Lim serves as an Associate Editor for the *IET Electric Power Applications*.



Felipe Bovolini Grigoletto (Member, IEEE) was born in Restinga Seca, Brazil, in 1985. He received the B.Sc., M.Sc., and D.Sc. degrees in electrical engineering from the Federal University of Santa Maria, Santa Maria, Brazil, in 2007, 2009, and 2013, respectively.

He is currently a Professor with the Federal University of Pampa (UNIPAMPA), Alegrete, Brazil. His current research interests include modulation and control strategies for power converters, multilevel topologies, grid-connected converters, and renewable energy conversion systems.



Yam Prasad Siwakoti (Senior Member, IEEE) received the B.tech. degree in electrical engineering from the National Institute of Technology, Hamirpur, India, in 2005, the M.Eng. degree in electrical power engineering from the Norwegian University of Science and Technology, Trondheim, Norway, and Kathmandu University, Dhulikhel, Nepal, in 2010, and the Ph.D. degree in electronics engineering with a specialization in power electronics from Macquarie University, Sydney, NSW, Australia, in 2014.

He was a Postdoctoral Fellow with the Department of Energy Technology, Aalborg University, Aalborg, Denmark, from 2014 to 2016. He was a Visiting Scientist with the Fraunhofer Institute for Solar Energy Systems, Freiburg, Germany, from 2017 to 2018. He is currently a Senior Lecturer with the Faculty of Engineering and Information Technology, University of Technology Sydney, Sydney, NSW, Australia.

Dr. Siwakoti was a recipient of the Fraunhofer Bessel Research Award from Alexander von Humboldt Foundation, Germany, in 2022, Champion of IEEE IES Inter-Chapter Paper Competition in 2021, and Green Talent Award from the Federal Ministry of Education and Research, Germany, in 2016. He served as an Associate Editor for the *IET Power Electronics* from 2015 to 2022. He is serving as an Associate Editor for IEEE TRANSACTIONS ON POWER ELECTRONICS, IEEE TRANSACTIONS ON INDUSTRIAL ELECTRONICS, and IEEE JOURNAL OF EMERGING AND SELECTED TOPICS IN POWER ELECTRONICS.